PNAS RESEARCH ARTICLE | CHEMISTRY BIOCHEMISTRY

Manipulating complex chromatin folding via CRISPR-guided bioorthogonal chemistry

Geng Qin[a,b,c], Jie Yang[a,b,c], Chuanqi Zhao[a,b,c], Jinsong Ren[a,b,c], and Xiaogang Qu[a,b,c,1]

Edited by Vivian Yam, University of Hong Kong, Hong Kong, China; received March 17, 2022; accepted August 2, 2022

Precise manipulation of chromatin folding is important for understanding the relationship between the three-dimensional genome and nuclear function. Existing tools can reversibly establish individual chromatin loops but fail to manipulate two or more chromatin loops. Here, we engineer a powerful CRISPR system which can manipulate multiple chromatin contacts using bioorthogonal reactions, termed the bioorthogonal reaction-mediated programmable chromatin loop (BPCL) system. The multiinput BPCL system employs engineered single-guide RNAs recognized by discrete bioorthogonal adaptors to independently and dynamically control different chromatin loops formation without cross-talk in the same cell or to establish hubs of multiway chromatin contacts. We use the BPCL system to successfully juxtapose the pluripotency gene promoters to enhancers and activate their endogenous expression. BPCL enables us to independently engineer multiway chromatin contacts without cross-talk, which provides a way to precisely dissect the high complexity and dynamic nature of chromatin folding.

3D genome | chromatin loop | CRISPR | bioorthogonal reaction | engineered sgRNAs

Mammalian genomic DNA can exceed 2 m in linear length (1). For adapting the cell nucleus, DNA does not exist as a linear molecule but instead is hierarchically packaged to form a chromatin fiber, which is subsequently folded into complex higher-order structures such as loops, domains, and compartments (2). Chromatin folding has been demonstrated to be involved in regulating many biological processes. For example, the formation of chromatin loops is frequently linked to long-distance gene regulation that in turn controls development and cell fate commitment (3), and abnormal chromatin loops formation may indicate a sign of disease (4, 5). Therefore, engineering of chromatin loops can help elucidate how chromatin loops provide spatiotemporal precision in transcriptional regulation. Recent progress on the development of tools based on zinc fingers (ZF) or CRISPR–nuclease-deactivated Cas9 (CRISPR-dCas9) has enabled controlling chromatin loop formation (6). Deng et al. developed a ZF strategy to induce chromatin looping by the ZF protein fused with the looping factor LDB to induce chromatin loop at the endogenous β-globin locus (7). Hao et al. used two orthogonal *Streptococcus pyogenes* (Sp) and *Streptococcus thermophilus* (St) dCas9 proteins that are fused with leucine zippers to establish a chromatin loop between the two endogenous genomic loci (8). To further enhance the operability of the tools for engineering chromatin loops, Morgan et al. and Kim et al., respectively, developed small ligand- or optogenetic-inducible CRISPR-based tools, chromatin loop reorganization using CRISPR-dCas9 (CLOuD9), and light-activated dynamic looping (LADL) (9, 10). However, all these reported tools can only manipulate individual chromatin loops, which has prohibited our ability to more precisely dissect the high complexity and dynamic nature of chromatin folding. The development of tools to engineer chromatin loops in a multiplexed and orthogonal fashion will help toward building a more thorough understanding of how DNA controls chromatin folding and how the latter underlies proper gene regulation. These potential insights would be of significant importance for deciphering the correlation between aberrations in three-dimensional genome and cell fate, generic diseases, and cancers.

Bioorthogonal chemistry has emerged as a powerful toolbox for dissecting complex biological processes in the native environment (11, 12). A series of chemical reactions that is orthogonal to most functional groups in living systems have shown great potential to regulate specific biological events (13, 14). The well-known examples of such reactions are the azide–alkyne cycloaddition and the inverse electron demand DielsAlder reaction, often referred to as "click" chemistry (15). Such bioorthogonal reactive groups can be engineered into a biomolecule, such as nucleic acids (16, 17), proteins (18), lipids (19, 20), and glycans (21, 22), without perturbing their biological function, enabling the selective installation of special tag or manipulation of the biomolecules in their native environment.

Significance

The development of tools to manipulate chromatin contacts in a multiplexed and orthogonal fashion will help toward building a more thorough understanding of how DNA controls chromatin folding and how the latter underlies proper gene regulation. However, existing tools can only manipulate chromatin contacts of two genomic loci. In this work, we developed a chromatin topology operating system by combing CRISPR and bioorthogonal chemistry, which can dynamically and orthogonally engineer chromatin contacts of multiple genomic loci. Future work with this system will better reveal the hierarchy and dynamics of the three-dimensional genome as well as how both de novo and orthogonal chromatin contacts of multiple genomic loci can be harnessed to alter transcriptional programs in development and disease.

Author affiliations: [a]State Key Laboratory of Rare Earth Resource Utilization, Changchun Institute of Applied Chemistry, Chinese Academy of Sciences, Changchun 130022, People's Republic of China; [b]Laboratory of Chemical Biology, Changchun Institute of Applied Chemistry, Changchun 130022, People's Republic of China; and [c]School of Applied Chemistry and Engineering, University of Science and Technology of China, Hefei 230026, People's Republic of China

Author contributions: J.R. and X.Q. designed research; G.Q. performed research; G.Q., J.Y., and C.Z. contributed new reagents/analytic tools; G.Q., J.Y., and C.Z. analyzed data; and G.Q. and X.Q. wrote the paper.

The authors declare no competing interest.

This article is a PNAS Direct Submission.

Copyright © 2022 the Author(s). Published by PNAS. This article is distributed under Creative Commons Attribution-NonCommercial-NoDerivatives License 4.0 (CC BY-NC-ND).

[1]To whom correspondence may be addressed. Email: xqu@ciac.ac.cn.

This article contains supporting information online at http://www.pnas.org/lookup/suppl/doi:10.1073/pnas.2204725119/-/DCSupplemental.

Published August 29, 2022.

Here, we present a bioorthogonal CRISPR system for regulating complex chromatin folding events, termed the bioorthogonal reaction-mediated programmable chromatin loop (BPCL) system. We have systematically explored three BPCL systems and optimized how dCas9 can deploy the clickable and photocleavable adaptors to the targeted genome loci by dynamically incorporating the adaptors into the single-guide RNAs (sgRNAs) scaffolds. By using two compatible bioorthogonal reactions strain promoted azide–alkyne cycloaddition (SPAAC) and strain-promoted inverse electron-demand DielsAlder cycloaddition (SPIEDAC), the system can dynamically regulate different chromatin loops formation without cross-talk in the same cell or establish the hubs of multiway chromatin contacts. By using the optimized system, we successfully juxtaposed the promoters of the pluripotency genes to their enhancers, enabling activation of their endogenous expression. BPCL enables the manipulation of chromatin folding in distinct regulatory patterns, and our work provides insights into highly specific and orthogonal control over multiple chromatin contacts by using bioorthogonal chemistry.

Results

Design and Implementation of the BPCL System. We designed the BPCL system in a modular manner with three key components. First, we engineered two sgRNAs respectively integrated with the adaptor target sequence 1 (ATS1) and ATS2 not found in the human genome (23). Second, these sgRNAs were used to recruit dCas9 at two different genomic target sites. Finally, we used single-stranded clickable oligonucleotide adaptors (ssCOAs), which were modified by SPAAC-reactive groups (azide or DBCO) as well as the photocleavable (PC) linker (*SI Appendix*, Fig. S1) as chromatin loop-induced agents (Fig. 1*A*). In principle, BPCL would reversibly manipulate chromatin loops via supplementation/photocleavage of the adaptors due to inducing dCas9/sgRNA complex dimerization by SPAAC ligation.

Engineering the recruitment sequences for proteins or nucleic acids into sgRNA scaffolds has been widely investigated to expand or optimize the CRISPR toolset (17, 23–25). We designed three different kinds of sgRNA scaffolds, each with the ATS appended into the sgRNA stem loop 2 (SL2-sgRNA), tetraloop (TL-sgRNA), and 3′ terminal end (3′-sgRNA) (*SI Appendix*, Tables S1 and S2). We generated three vectors including dCas9 and three different kinds of gRNAs, respectively, and named the resulting vectors BPCL 1.1, BPCL 1.2, and BPCL 1.3 (Fig. 1*B* and *SI Appendix*, Figs. S2–S4). We first determined whether the designed sgRNAs with supplementation of the adaptors were still functional. By performing chromatin immunoprecipitation (ChIP), we demonstrated strong enrichment of dCas9 at the target sites with supplementation of the single-stranded oligonucleotide adaptors (ssOAs, without bioorthogonal reactive group modification, as a control), but not a nonspecific genomic region (Fig. 1*C*), indicating the correct localization and targeting of each BPCL. Given that the dCas9/sgRNA CRISPR system can be used to visualize genomic repetitive sequences such as telomeres in living cells (26), we therefore explored whether the designed sgRNAs with supplementation of the adaptors affected the specificity and efficiency of telomere imaging by CRISPR. We performed two-color imaging with a dCas9-EGFP (enhanced green fluorescent protein) CRISPR system and immunofluorescence for endogenous TRF1, which is a protein that locates at the telomere region. The dCas9-EGFP was stably coexpressed with the designed sgRNAs targeting telomere in HeLa cells, and then ssOAs were added. The observed green CRISPR puncta colocalized with red TRF1 puncta in the cell nucleus (Fig. 1*D*), indicating successful telomere imaging by CRISPR. Collectively, these results indicated that the sgRNAs with supplementation of the adaptors did not influence the formation and genomic targeting of the dCas9/sgRNA complex.

Then, we studied whether SPAAC reaction could induce dCas9/sgRNA complex oligomerization. As expected, 5′-azide–modified ssCOAs can readily link with the 3′-DBCO–modified ssCOAs via SPAAC reaction in vitro (Fig. 1*E*). Furthermore, we stably coexpressed dCas9-EGFP with the negative sgRNAs in BPCL 1.2–engineered HeLa cells and then added ssCOAs whose two terminal ends were modified with azide or DBCO (*SI Appendix*, Fig. S5*A*). We found that addition of these ssCOAs produced increased green CRISPR puncta numbers as well as decreased background, and this effect could be reversed in response to light illumination (*SI Appendix*, Fig. S5 *B* and *C*). It is worth noting that the efficiency of ssCOAs in vivo annealing and bioorthogonal ligation exceeded 80% (*SI Appendix*, Fig. S5*D*). These results demonstrated that the ssCOAs-mediated SPAAC reaction could induce the dCas9-EGFP/sgRNA complex oligomerization and ultraviolet light could dissociate the complex oligomerization.

Implementing the Manipulation of a Single Chromatin Loop. It has been reported that the formation of chromatin loops that juxtapose the enhancer and promoter regions is a critical epigenetic barrier to activate endogenous pluripotent genes (27) such as *POU5F1* (also called *OCT4*), *NANOG*, and *SOX2*, etc. We next chose to first test the utility of BPCL on the human *POU5F1* locus. The contact of *POU5F1* promoter and 3′ enhancer is necessary for driving transcription of *POU5F1* in embryonic stem cells (27), and thus we targeted the BPCL anchor to the *POU5F1* promoter and 3′ enhancer in HEK293T cells where there is no endogenous interaction (Fig. 2*A*). The HEK293T cells were stably expressed in BPCL systems after puromycin selection, and then we added the dual-ssOAs (as a control) or photocleavable dual-ssCOAs (azide-PC linker-modified ssCOAs and DBCO-modified ssCOAs) to reversibly induce chromatin loops formation (Fig. 2*B*).

We first confirmed the correct localization of each BPCL system (*SI Appendix*, Fig. S6 *A*–*C*). In addition, by performing chromosome conformation capture (3C) methodology to investigate the chromatin structure surrounding the *POU5F1* gene, we detected high-frequency interactions between *POU5F1* promoter and 3′ enhancer (A1–A6) in dual-ssCOAs groups but not in any control groups and the dual-ssCOAs groups with light illumination (Fig. 2 *C*–*E* and *SI Appendix*, Fig. S7 *A*–*C*). BPCL 1.2 mediated the largest increase in the frequency of the A1–A6 interaction, and the median frequency of the A1–A6 interaction increased ∼1.3-fold and ∼1.5-fold in BPCL 1.2 groups versus BPCL 1.1 groups and BPCL 1.3 groups, respectively (Fig. 2*F*). It is worth noting that we observed that BPCL could induce comparable cross-link frequency compared with CLOuD9, which is an existing chromatin loop operating system based on small ligand-inducible CRISPR (*SI Appendix*, Fig. S8). Finally, we found that a sufficient length of sequence flanking the ATS was essential for effective manipulation of chromatin loop with BPCL (*SI Appendix*, Fig. S9 *A* and *B*).

To investigate the detailed dynamic characterizations of BPCL systems, we monitored A1–A6 contacts over 6 d in BPCL 1.2–engineered HEK293T cells. We found that cells upon continuous dual-ssCOAs treatment maintained high-frequency A1–A6 interactions over 6 d (Fig. 2*G*). Removal of the dual-ssCOAs or illumination by light could lead to a decrease in A1–A6 contact frequency, even down to the baseline

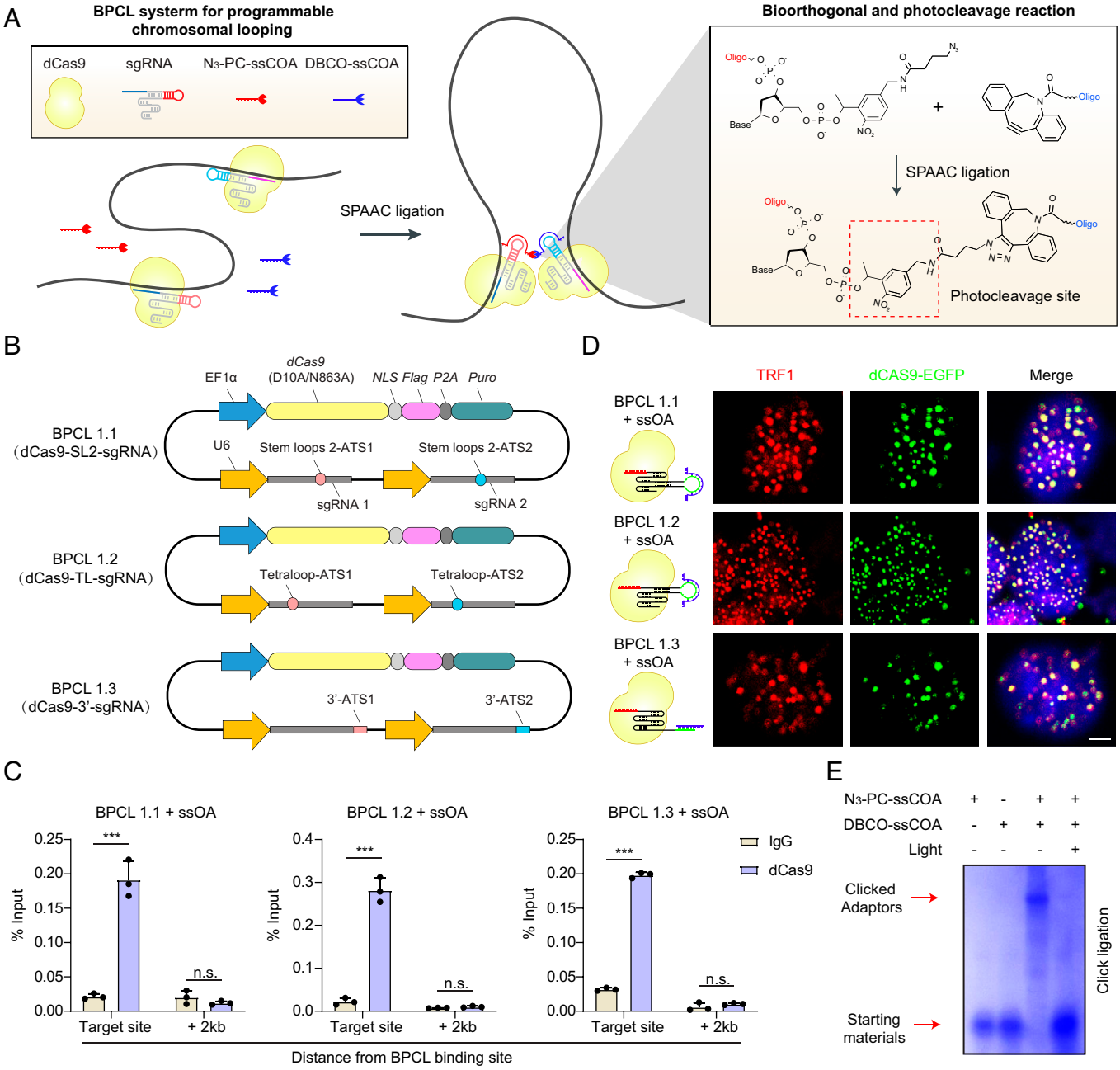

Fig. 1. Design and implementation of the BPCL system. (*A*) Schematic diagrams of the BPCL system. (*B*) Design of three lentiviral vectors for expressing dCas9 and three kinds of engineered sgRNAs. Each vector contains a puromycin selectable marker to enable the selection of cells expressing these vectors. (*C*) Chromatin immunoprecipitation and quantitative real-time PCR (ChIP-qRT-PCR) assays of BPCL constructs demonstrates correct localization to their intended genomic loci. Data are shown as mean ± SEM of three independent experiments, two-tailed Student's *t* test. n.s., not significant. ***$P < 0.001$. (*D*) Detection of telomere loci by dCas9-EGFP/sgRNA/adaptors complexes and the immunofluorescence (IF) assay of TRF1. (Scale bar, 4 μm.) (*E*) Azide- and DBCO-modified adaptors can link together in vitro via SPAAC and be cleaved by ultraviolet light illumination.

in 3 d or 1 d, respectively (Fig. 2*H*); this indicated the reversibility of chromatin loop formation by BPCL. In addition, readdition of dual-ssCOAs in these cells could induce the A1–A6 contacts as strongly and rapidly as the original treatment (Fig. 2*H*). It is noteworthy that BPCL could significantly induce the A1–A6 contacts just after 6 h of addition of dual-ssCOAs (*SI Appendix*, Fig. S10 *A* and *B*). We also investigated the impacts of long-term induced chromatin loop by using BPCL (*SI Appendix*, Fig. S11*A*). After 10 d of addition of dual-ssCOAs, we still detected high-frequency A1–A6 interactions in dual-ssCOAs groups, but it could not be completely reversed in response to light illumination (*SI Appendix*, Fig. S11*B*). It has been demonstrated that the cohesin-complex gene SMC1 is essential for maintenance of chromatin loop (27), and thus we hypothesized that long-term induced chromatin loop may recruit the SMC1 to maintain the contact. Indeed, addition of dual-ssCOAs caused a significant increase in the strength of SMC1 binding at the *POU5F1* 3′ enhancer and promoter, and light illumination showed no noticeable effects on their interactions (*SI Appendix*, Fig. S11*C*). Collectively, our results indicated that BPCL could flexibly manipulate the chromatin on different time scales.

Given that the contact of 3′ enhancer and the promoter is critical for *POU5F1* endogenous transcriptional activation, we next investigated the effects of the BPCL-engineered promoter and enhancer interactions on *POU5F1* expression. As expected, the RNA levels of *POU5F1* were significantly increased in

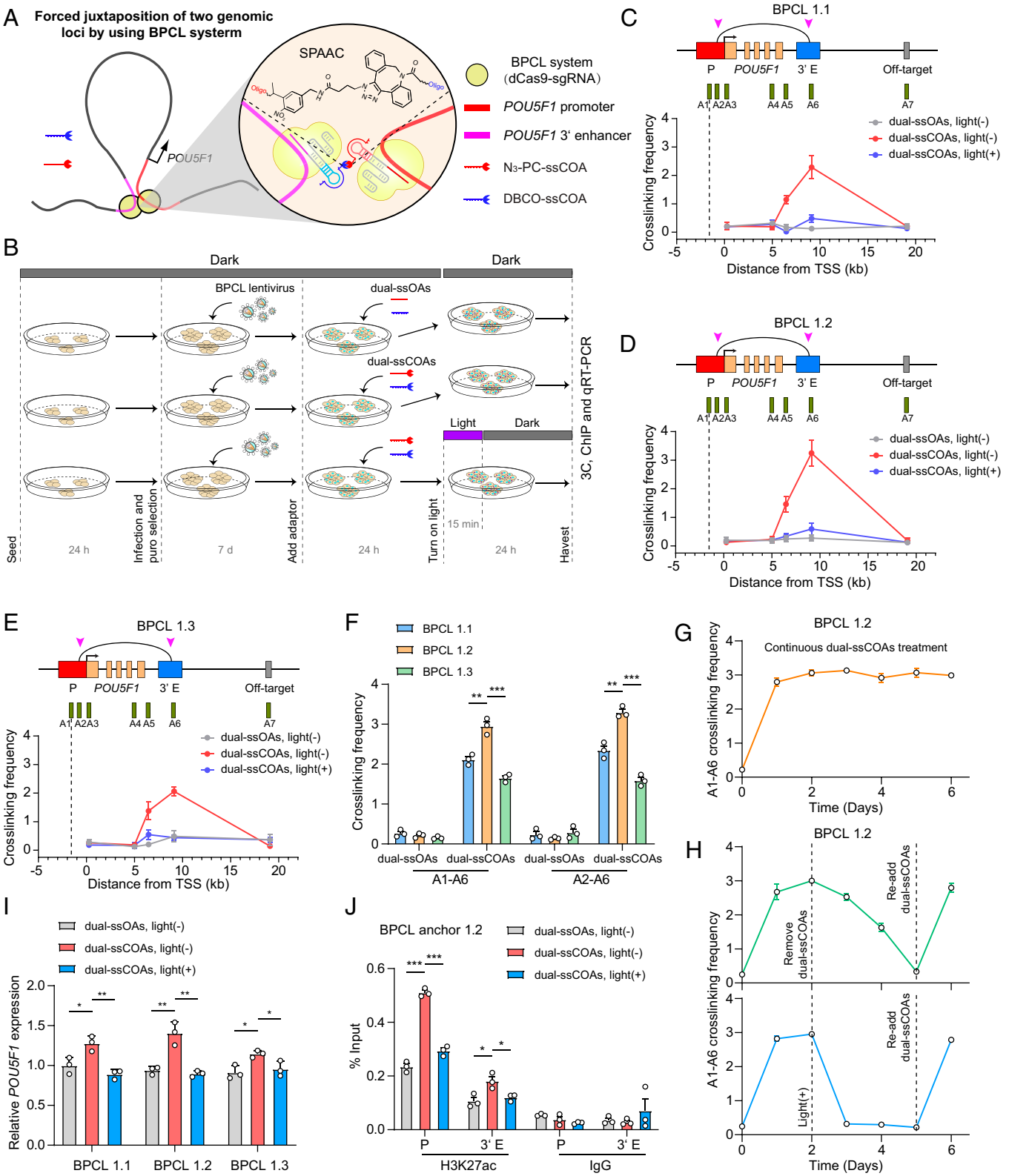

Fig. 2. BPCL induces reversible interaction between *POU5F1* promoter and 3′ enhancer. (*A*) Schematic diagram of forced juxtaposition of *POU5F1* promoter and 3′ enhancer by the BPCL system. (*B*) Schematic timeline of seeding, lentiviral infection, puromycin selection, adding adaptors, light illumination, and harvest of HEK293T cells. (*C*–*E*) Chromosome conformation capture (3C) assays measuring *POU5F1* locus-wide cross-linking frequencies in BPCL 1.1– (*C*), BPCL 1.2– (*D*) and BPCL 1.3– (*E*) engineered HEK293T cells without or with dual-ssOAs, dual-ssCOAs and light illumination. ssOAs, single-stranded oligonucleotide adaptors; ssCOAs, single-stranded clickable oligonucleotide adaptors; dual-ssCOAs, azide-PC linker-modified ssCOAs and DBCO-modified ssCOAs. (*F*) The cross-linking frequencies between the *POU5F1* promoter and 3′enhancer (A1–A6 and A2–A6) regions in BPCL 1.1–, BPCL 1.2–, and BPCL 1.3–engineered HEK293T cells. (*G* and *H*) Characterization of the dynamics of dual-ssCOAs-inducible *POU5F1* promoter-3′enhancer loop formation. BPCL 1.2–engineered HEK293T cells were continuously induced with dual-ssCOAs for 6 d (*G*), induced for 2 d, then cultured without dual-ssCOAs for 3 d then reinduced for 1 d (*H*, *Top*) or induced for 2 d, cultured for 3 d after light illumination, then reinduced for 1 d (*H*, *Bottom*). (*I*) The relative expression of *POU5F1* in BPCL 1.1–, BPCL 1.2–, and BPCL 1.3–engineered HEK293T cells, detected by qRT-PCR. (*J*) ChIP-qRT-PCR demonstrates reversible alterations in H3K27ac at the promoter and 3′ enhancer regions of *POU5F1*in BPCL 1.2–engineered HEK293T cells. Data are shown as mean ± SEM of three independent experiments, two-tailed Student's *t* test. **P* < 0.05, ***P* < 0.01, ****P* < 0.001.

BPCL-engineered HEK293T cells after the addition of dual-ssCOAs, with baseline levels being restored in response to light illumination (Fig. 2*I*). Consistent with 3C results, BPCL could induce comparable increase of *POU5F1* RNA levels compared with CLOuD9 (*SI Appendix*, Fig. S12). It is worth noting that despite that A1–A6 interactions in BPCL 1.2–engineered cells upon continuous dual-ssCOAs treatment over 6 d were not further increased, the RNA levels of *POU5F1* were gradually increased in a time-dependent manner (*SI Appendix*, Fig. S13), suggesting that long-term continuous induction of high-frequency interaction can further increase the expression of *POU5F1*. In support of these observations, addition of dual-ssCOAs specifically increased the histone 3 lysine 27 acetylation (H3K27ac) levels, which is associated with active transcription, at the promoter and enhancer region of *POU5F1* (Fig. 2*J* and *SI Appendix*, Fig. S14 *A* and *B*). For long-term induced chromatin loop, the same results were found in the studies of the *POU5F1* RNA levels and the H3K27ac in *POU5F1* 3′ enhancer and promoter regions (*SI Appendix*, Fig. S15 *A* and *B*). However, the BPCL-mediated interactions between *POU5F1* promoter and the nonenhancer region could not change the RNA and H3K27ac levels (*SI Appendix*, Fig. S16 *A*–*C*). Taken together, BPCL could activate *POU5F1* transcription by inducing the contact of *POU5F1* enhancer and promoter.

Orthogonal Manipulation of Different Chromatin Loops via the BPCL System. To increase the flexibility and scope of the BPCL system, we added a second, independent bioorthogonal chemical reaction to allow simultaneous and orthogonal manipulation of different chromatin loops. It has been reported that SPAAC and SPIEDAC are two compatible bioorthogonal reactions without cross-talk between them (28). Thus, we chose the SPIEDAC reaction and verified whether SPIEDAC reactive groups (methyltetrazine or TCO) modified ssCOAs could manipulate the chromatin loop (*SI Appendix*, Figs. S1, S17, and S18*A*). As expected, addition of SPIEDAC-ssCOAs significantly increased the frequency of the A1–A6 interaction in BPCL 1.2–engineered cells (*SI Appendix*, Fig. S18*B*). It is noteworthy that SPIEDAC-ssCOAs could also quickly enable the formation of chromatin loop on demand (*SI Appendix*, Fig. S18*C*). Consistent with our observations by using SPAAC reaction, addition of SPIEDAC-ssCOAs could activate *POU5F1* transcription (*SI Appendix*, Fig. S18*D*).

Next, we used these two compatible bioorthogonal reactions to demonstrate simultaneous and independent regulation of two chromatin loops by the BPCL system. We engineered the BPCL 2.1 system including dCas9 and four sgRNAs, respectively, integrated with ATS1–4, and azide-, DBCO-, methyltetrazine-, or TCO-modified ssCOAs that target respectively ATS1 through ATS4 (Fig. 3 *A* and *B* and *SI Appendix*, Fig. S19). As expected,

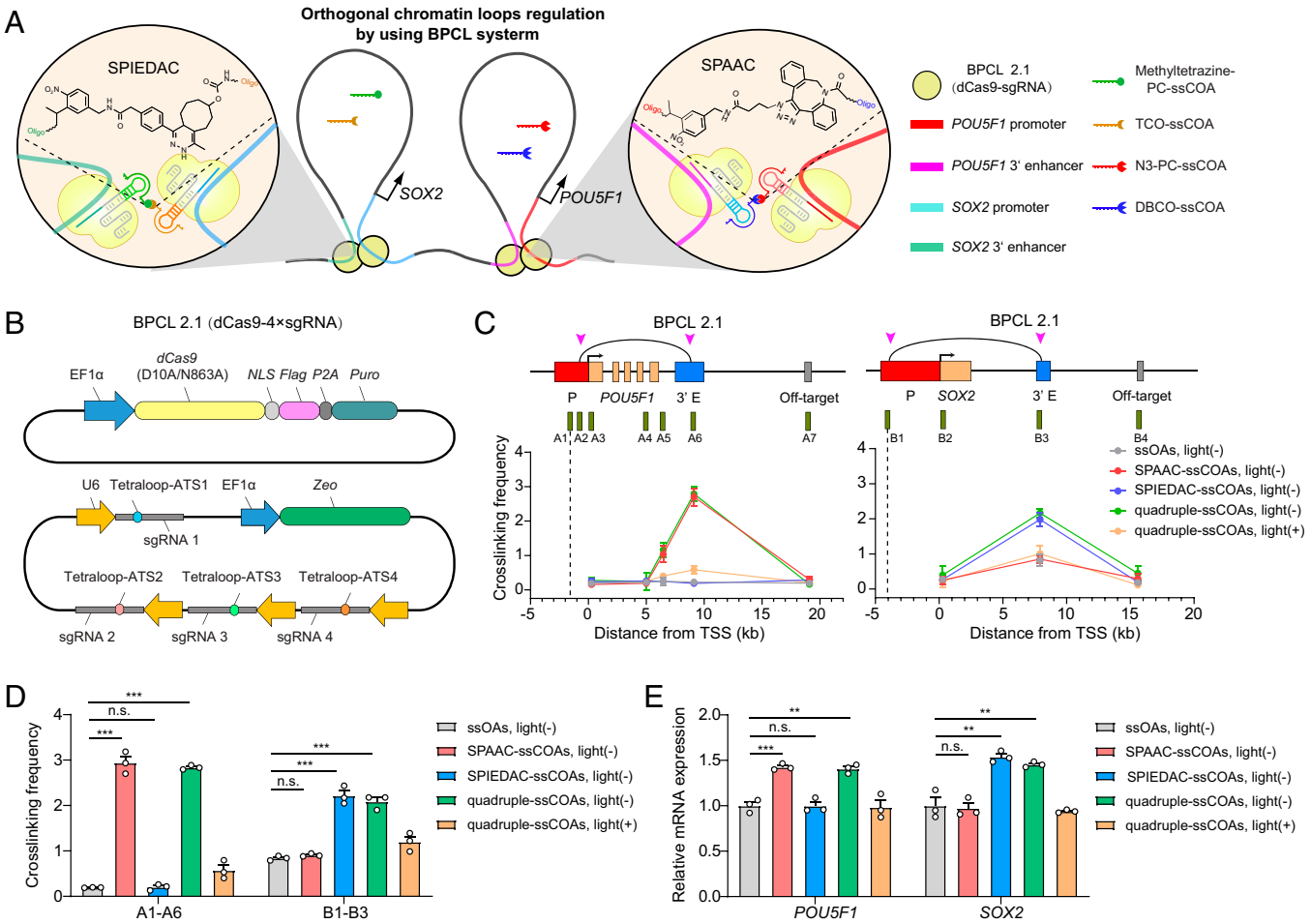

Fig. 3. Orthogonal chromatin loops regulation via BPCL. (*A*) The schematic diagram of orthogonal regulation of *POU5F1* and/or *SOX2* promoter–enhancer contacts by the BPCL system. (*B*) Design of two lentiviral vectors for expressing dCas9 and four engineered sgRNAs. Each vector contains a distinct selection marker to enable coselection of cells expressing both vectors. (*C*) The 3C assays measuring *POU5F1* (*Left*) and *SOX2* (*Right*) locus-wide cross-linking frequencies in BPCL 2.1–engineered HEK293T cells without or with ssOAs, SPAAC-ssCOAs, SPIEDAC-ssCOAs, quadruple-ssCOAs and light illumination, quadruple-ssCOAs, SPAAC-ssCOAs, and SPIEDAC-ssCOAs. (*D*) The cross-linking frequencies of *POU5F1* and *SOX2* promoter–3′enhancer (A1–A6 and B1–B3) in BPCL 2.1–engineered HEK293T cells. (*E*) The relative expression of *POU5F1* and *SOX2* in BPCL 2.1–engineered HEK293T cells, detected by qRT-PCR. Data are shown as mean ± SEM of three independent experiments, two-tailed Student's *t* test. n.s., not significant. $^{**}P < 0.01$, $^{***}P < 0.001$.

SPAAC- and SPIEDAC-ssCOAs could independently or simultaneously trigger *POU5F1* promoter-3′ enhancer (A1–A6) and *SOX2* promoter-3′ enhancer (B1–B3) contacts in BPCL 2.1–engineered HEK293T cells (Fig. 3 *C* and *D*), which in turn activated the transcription of *POU5F1* and *SOX2* (Fig. 3*E*). Flow cytometry analysis showed that under induction by both SPAAC- and SPIEDAC-ssCOAs, individual cells simultaneously expressed higher levels of *POU5F1* and *SOX2* (*SI Appendix*, Fig. S20), suggesting that BPCL 2.1 system can act in one cell in an orthogonal fashion. By using the BPCL 2.1 system, we also could up-regulate the RNA levels of *SOX2* and *NANOG* by independently or simultaneously inducing the promoter–enhancer contact of *SOX2* and *NANOG* (*SI Appendix*, Fig. S21). Thus, these results suggested that the upgraded BPCL could flexibly manipulate the different chromatin loops without cross-talk in the same cell.

Establishing Hubs of Multiway Chromatin Contacts via a Multiinput BPCL System. For exploring the BPCL system to manipulate the spatial connection of three genomic loci (Fig. 4*A*), another sgRNA (SL2-TL-sgRNA) with ATS1 and ATS3, respectively, appended into the sgRNA stem loop 2 and tetraloop was designed (*SI Appendix*, Table S1). We generated the vector including the dCas9, SL2-TL-sgRNA, TL-sgRNA-ATS2, and TL-sgRNA-ATS4 and named the resulting vectors BPCL 3.1 (Fig. 4*B* and *SI Appendix*, Fig. S22). As the 5′ distal enhancer is juxtaposed to the *POU5F1* promoter/3′ enhancer complex during endogenous gene activation (9), we assessed whether addition of quadruple-ssCOAs (four kinds of ssCOAs respectively modified by azide, DBCO, methyltetrazine, and TCO) can regulate the interactions among *POU5F1* promoter, 3′ enhancer and 5′ distal enhancer regions. As expected, we detected high-frequency promoter-3′ enhancer (A1–A6) and promoter-5′ distal enhancer (A0–A1) interactions in quadruple-ssCOAs groups but not in the control groups and the quadruple-ssCOAs groups with light illumination (Fig. 4*C*). It is noteworthy that we could arbitrarily regulate the pairwise interactions of three genomic loci by adding the different input for combination of ssCOAs (Fig. 4*D*). We observed that BPCL 3.1–engineered cells just added with SPAAC-ssCOAs showed an increase in the frequency of A1–A6 contact, and the cells added with SPIEDAC-ssCOAs exhibited an increase in A0–A1 interaction frequency. Addition of both SPAAC- and SPIEDAC-ssCOAs could induce the interactions between the three regions (Fig. 4*E*). Furthermore, we found that the RNA levels of *POU5F1* could be increased by adding SPAAC- and SPIEDAC-ssCOAs independently or simultaneously, and addition of both SPAAC- and SPIEDAC-ssCOAs mediated the largest increase in RNA levels of *POU5F1* (*SI Appendix*, Fig. S23). Consistently, BPCL 3.1 could further activate the transcription of *POU5F1* compared with BPCL 1.2 (*SI Appendix*, Fig. S24). Collectively, our designed BPCL system can operate multiple input signals to manipulate complex dynamic chromatin folding events.

Discussion

Inspired by the advantages of bioorthogonal chemistry, we have designed a dCas9-based chromatin topology operating system for manipulation of chromatin loops by integration of bioorthogonal clicking reactions. Via engineering the sgRNA to incorporate the adaptor target sequences, each pair of dCas9/sgRNA complexes is designed with matched discrete bioorthogonal reaction groups modified adaptors. This will allow us to 1) simultaneously engineer different chromatin loops without cross-talk in the same cell and 2) flexibly establish the hubs of multiway chromatin contacts. The BPCL system used bioorthogonal clicking

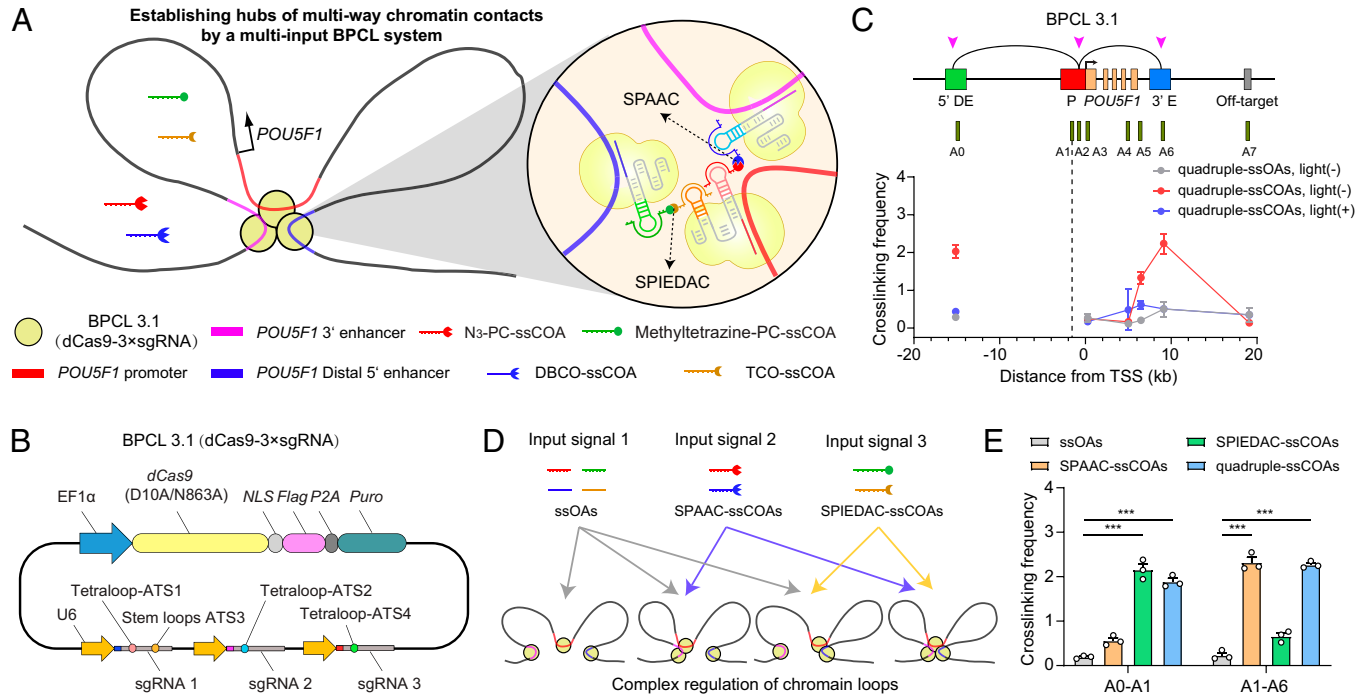

Fig. 4. A multiinput BPCL system for complex regulation of chromain loops. (*A*) The schematic diagram of forced juxtaposition of three genomic loci (*POU5F1* promoter, distal 5′ enhancer, and 3′ enhancer regions) by the BPCL system. (*B*) Design of the lentiviral vector for expressing dCas9 and three engineered sgRNAs. (*C*) The 3C assays measuring *POU5F1* locus-wide cross-linking frequencies in BPCL 3.1–engineered HEK293T cells without or with ssOAs, quadruple-ssCOAs, and light illumination. (*D*) The schematic diagram of complex regulation of three genomic loci contacts by a multiinput BPCL system. (*E*) The cross-linking frequencies of *POU5F1* promoter–distal 5′ enhancer (A0–A1) and promoter–3′enhancer (A1–A6) in BPCL 3.1–engineered HEK293T cells. Data are shown as mean ± SEM of three independent experiments, two-tailed Student's *t* test. ***$P < 0.001$.

reactions instead of small ligand- or light-inducible heterodimerization structural domains to spatially connect the different genomic loci, which may mitigate to the maximum potential effects on nuclear environments. Moreover, due to the better operability and flexibility of BPCL on genome folding, future work with BPCL could further facilitate ongoing efforts to engineer structural loops and enhancer–promoter loops, gaining a deep understanding of how chromatin looping provides spatiotemporal precision in transcriptional regulation.

Pluripotency genes connect to their target enhancers through long-range interactions, which is essential for their transcriptional activation (29–31). Due to the absence of these long-range interactions in somatic cells, generation of induced pluripotent stem cells by defined factors (OCT4, SOX2, KLF4, and c-MYC) is an extremely inefficient process (27). In this study, we used the BPCL system to independently reprogram specific contacts between these genes such as *POU5F1*, *SOX2*, and *NANOG* and target enhancers in the cells where there is no endogenous interaction, leading to the transcription activation of these pluripotency genes. Meanwhile, we confirmed that the simultaneous multivalent contacts of *POU5F1* promoter, 3′ enhancer, and distal 5′ enhancer can further drive the transcription of *POU5F1*, supporting the critical roles of chromatin folding in the control of pluripotency and cellular differentiation.

We envision that the BPCL system can be expanded into a "plug-and-play" toolbox to increase the numbers of chromatin loops simultaneously manipulated in the future by introducing more compatible bioorthogonal reactions, increasing the bioorthogonal groups numbers of single dCas9/sgRNA complexes, and designing adaptor structure or adjusting sgRNA numbers. These may enable design of complex chromatin contacts to build disease models for understanding a cause-and-effect relationship between chromatin misfolding and occurrence of genetic disease. Our work provides insights into CRISPR-guided bioorthogonal chemistry for correcting abnormal chromatin folding or reprogramming the genome architecture in disease.

Materials and Methods

The ChIP and immunofluorescence assays were used to confirm the correct localization of each BPCL systems. Chromosome conformation capture (3C) methodology was used to investigate the chromatin structure surrounding the *POU5F1*, *SOX2*, and *NANOG* loci. Flow cytometry and quantitative real-time PCR assays were used to detect the gene expression. Detailed material and methods descriptions can be found in *SI Appendix, SI Materials and Methods*.

Data, Materials, and Software Availability. All study data are included in the article and/or *SI Appendix*.

ACKNOWLEDGMENTS. Financial support was provided by the National Key R&D Program of China (2019YFA0709202 and 2021YFF1200700), the National Natural Science Foundation of China (91856205, 21820102009, 21871249, 22107098, and 22122704), and the Key Program of Frontier of Sciences (CAS QYZDJ-SSW-SLH052).

1. D. Zhang, J. Lam, G. A. Blobel, Engineering three-dimensional genome folding. *Nat. Genet.* **53**, 602–611 (2021).
2. E. H. Finn, T. Misteli, Molecular basis and biological function of variability in spatial genome organization. *Science* **365**, eaaw9498 (2019).
3. D. U. Gorkin, D. Leung, B. Ren, The 3D genome in transcriptional regulation and pluripotency. *Cell Stem Cell* **14**, 762–775 (2014).
4. D. G. Lupiáñez, M. Spielmann, S. Mundlos, Breaking TADs: How alterations of chromatin domains result in disease. *Trends Genet.* **32**, 225–237 (2016).
5. J. H. Ahn *et al.*, Phase separation drives aberrant chromatin looping and cancer development. *Nature* **595**, 591–595 (2021).
6. H. Wang, M. Han, L. S. Qi, Engineering 3D genome organization. *Nat. Rev. Genet.* **22**, 343–360 (2021).
7. W. Deng *et al.*, Controlling long-range genomic interactions at a native locus by targeted tethering of a looping factor. *Cell* **149**, 1233–1244 (2012).
8. N. Hao, K. E. Shearwin, I. B. Dodd, Programmable DNA looping using engineered bivalent dCas9 complexes. *Nat. Commun.* **8**, 1628 (2017).
9. S. L. Morgan *et al.*, Manipulation of nuclear architecture through CRISPR-mediated chromosomal looping. *Nat. Commun.* **8**, 15993 (2017).
10. J. H. Kim *et al.*, LADL: Light-activated dynamic looping for endogenous gene expression control. *Nat. Methods* **16**, 633–639 (2019).
11. M. Boyce, C. R. Bertozzi, Bringing chemistry to life. *Nat. Methods* **8**, 638–642 (2011).
12. T. Carell, M. Vrabel, Bioorthogonal chemistry–Introduction and overview [corrected]. *Top. Curr. Chem. (Cham)* **374**, 9 (2016).
13. E. M. Sletten, C. R. Bertozzi, Bioorthogonal chemistry: Fishing for selectivity in a sea of functionality. *Angew. Chem. Int. Ed. Engl.* **48**, 6974–6998 (2009).
14. J. Li, P. R. Chen, Development and application of bond cleavage reactions in bioorthogonal chemistry. *Nat. Chem. Biol.* **12**, 129–137 (2016).
15. C. G. Parker, M. R. Pratt, Click chemistry in proteomic investigations. *Cell* **180**, 605–632 (2020).
16. N. Klöcker, F. P. Weissenboeck, A. Rentmeister, Covalent labeling of nucleic acids. *Chem. Soc. Rev.* **49**, 8749–8773 (2020).
17. J. T. George *et al.*, Terminal uridylyl transferase mediated site-directed access to clickable chromatin employing CRISPR-dCas9. *J. Am. Chem. Soc.* **142**, 13954–13965 (2020).
18. Y. Zhang, K. Y. Park, K. F. Suazo, M. D. Distefano, Recent progress in enzymatic protein labelling techniques and their applications. *Chem. Soc. Rev.* **47**, 9106–9136 (2018).
19. M. D. Best, M. M. Rowland, H. E. Bostic, Exploiting bioorthogonal chemistry to elucidate protein-lipid binding interactions and other biological roles of phospholipids. *Acc. Chem. Res.* **44**, 686–698 (2011).
20. T. W. Bumpus, J. M. Baskin, Greasing the wheels of lipid biology with chemical tools. *Trends Biochem. Sci.* **43**, 970–983 (2018).
21. S. T. Laughlin, C. R. Bertozzi, Metabolic labeling of glycans with azido sugars and subsequent glycan-profiling and visualization via Staudinger ligation. *Nat. Protoc.* **2**, 2930–2944 (2007).
22. T. L. Hsu *et al.*, Alkynyl sugar analogs for the labeling and visualization of glycoconjugates in cells. *Proc. Natl. Acad. Sci. U.S.A.* **104**, 2614–2619 (2007).
23. X. Wu *et al.*, A CRISPR/molecular beacon hybrid system for live-cell genomic imaging. *Nucleic Acids Res.* **46**, e80 (2018).
24. D. M. Shechner, E. Hacisuleyman, S. T. Younger, J. L. Rinn, Multiplexable, locus-specific targeting of long RNAs with CRISPR-display. *Nat. Methods* **12**, 664–670 (2015).
25. J. G. Zalatan *et al.*, Engineering complex synthetic transcriptional programs with CRISPR RNA scaffolds. *Cell* **160**, 339–350 (2015).
26. B. Chen *et al.*, Dynamic imaging of genomic loci in living human cells by an optimized CRISPR/Cas system. *Cell* **155**, 1479–1491 (2013).
27. H. Zhang *et al.*, Intrachromosomal looping is required for activation of endogenous pluripotency genes during reprogramming. *Cell Stem Cell* **13**, 30–35 (2013).
28. J. S. Italia *et al.*, Mutually orthogonal nonsense-suppression systems and conjugation chemistries for precise protein labeling at up to three distinct sites. *J. Am. Chem. Soc.* **141**, 6204–6212 (2019).
29. E. Apostolou *et al.*, Genome-wide chromatin interactions of the Nanog locus in pluripotency, differentiation, and reprogramming. *Cell Stem Cell* **12**, 699–712 (2013).
30. M. Denholtz *et al.*, Long-range chromatin contacts in embryonic stem cells reveal a role for pluripotency factors and polycomb proteins in genome organization. *Cell Stem Cell* **13**, 602–616 (2013).
31. Z. Wei *et al.*, Klf4 organizes long-range chromosomal interactions with the oct4 locus in reprogramming and pluripotency. *Cell Stem Cell* **13**, 36–47 (2013).